Ultrathin, Molecular-Sieving Graphene Oxide Membranes for Selective Hydrogen Separation

Hang Li *et al.*

Science **342**, 95 (2013);
DOI: 10.1126/science.1236686

Science (print ISSN 0036-8075; online ISSN 1095-9203) is published weekly, except the last week in December, by the American Association for the Advancement of Science, 1200 New York Avenue NW, Washington, DC 20005.

20. L. J. Cote, F. Kim, J. X. Huang, *J. Am. Chem. Soc.* **131**, 1043–1049 (2009).
21. A. Torrisi, C. Mellot-Draznieks, R. G. Bell, *J. Chem. Phys.* **132**, 044705 (2010).
22. M. B. Rao, S. Sircar, *J. Membr. Sci.* **85**, 253–264 (1993).
23. H. B. Park *et al*., *Science* **318**, 254–258 (2007).
24. I. Pinnau, W. J. Koros, *Ind. Eng. Chem. Res.* **30**, 1837–1840 (1991).
25. N. Y. Du *et al*., *Nat. Mater.* **10**, 372–375 (2011).
26. D. Shekhawat, D. R. Luebke, H. W. Pennline, "A review of carbon dioxide selective membranes: A topical report" (Report DOE/NETL 2003/1200, U.S. Department of Energy, National Energy Technology Laboratory, Pittsburgh, PA, 2003).
27. J. C. Poshusta, R. D. Noble, J. L. Falconer, *J. Membr. Sci.* **186**, 25–40 (2001).
28. S. Eigler, C. Dotzer, A. Hirsch, M. Enzelberger, P. Muller, *Chem. Mater.* **24**, 1276–1282 (2012).
29. M. B. Shiflett, H. C. Foley, *Science* **285**, 1902–1905 (1999).
30. R. M. de Vos, H. Verweij, *Science* **279**, 1710–1711 (1998).

Acknowledgments: This work was mainly supported by Korea Carbon Capture and Sequestration Research and Development Center (KCRC) (grant no. 2012-0008907) funded by the Korea government (Ministry of Science, Information Communication Technology and Future Planning). We thank the National Synchrotron Light Source at Brookhaven National Laboratory for providing the X9 beam line (grant no. DE-AC02-98CH10886) and B. D. McCloskey for thoughtful reading and commentary on our paper. H.B.P. also acknowledges support by the research fund of Hanyang University (grant no. 200900000001052).

Supplementary Materials
www.sciencemag.org/content/342/6154/91/suppl/DC1
Materials and Methods
Figs. S1 to S10
References (*31*, *32*)

4 February 2013; accepted 4 September 2013
10.1126/science.1236098

Ultrathin, Molecular-Sieving Graphene Oxide Membranes for Selective Hydrogen Separation

Hang Li,[1,2] Zhuonan Song,[1,2] Xiaojie Zhang,[1,2] Yi Huang,[1,2] Shiguang Li,[3] Yating Mao,[1] Harry J. Ploehn,[1] Yu Bao,[4] Miao Yu[1,2]*

Ultrathin, molecular-sieving membranes have great potential to realize high-flux, high-selectivity mixture separation at low energy cost. Current microporous membranes [pore size < 1 nanometer (nm)], however, are usually relatively thick. With the use of current membrane materials and techniques, it is difficult to prepare microporous membranes thinner than 20 nm without introducing extra defects. Here, we report ultrathin graphene oxide (GO) membranes, with thickness approaching 1.8 nm, prepared by a facile filtration process. These membranes showed mixture separation selectivities as high as 3400 and 900 for H_2/CO_2 and H_2/N_2 mixtures, respectively, through selective structural defects on GO.

Zeolites (*1*, *2*), silica (*3*), carbon (*4*), and polymers (*5*) have been made into microporous membranes that have shown promising gas mixture separation performance. These membranes separate mixtures on the basis of selective adsorption, diffusion rate differences, or molecular-sieving mechanisms. Current microporous membranes, however, are usually thicker than 20 nm to minimize undesirable flux contribution through nonselective membrane defects, and they maintain reasonably high separation selectivity.

Graphene-based materials, such as graphene and graphene oxide (GO), have been considered promising membrane materials, because they are only one carbon atom thick and, thus, may form separation membranes that minimize transport resistance and maximize flux. Additionally, they have good stability (*6*, *7*) and are mechanically strong (*8*). Graphene-based materials have been made into centimeter-sized, thick (~1-μm) membranes and micrometer-sized, isolated single sheets for pure component permeation studies where they were found to be either impermeable to small gas molecules or not practical for separation applications (*9*–*12*).

We used single-layered GO flakes, prepared by the modified Hummer's method (*13*). Ultrathin GO membranes were prepared by vacuum filtration, as described in detail in fig. S1. Centrifugation and dilution of GO dispersions were found to be important for preparing high-quality GO membranes [fig. S2 and discussion in (*13*)]. Figure 1A shows a ~9-nm-thick GO membrane with a permeation area of ~4 cm^2 on anodic aluminum oxide (AAO) support. A glass membrane module was used for gas permeation-separation experiments, as shown schematically in fig. S3. X-ray diffraction shows the characteristic peak of GO at 2θ of 11.1° [fig. S4 and analysis in (*13*)], and GO flakes are ~500 nm in size and single-layered, as confirmed by atomic force microscopy (AFM) (Fig. 1B), which also shows the height profile of a GO flake (Fig. 1C). In Fig. 1, panels D and E show the surface of an 18-nm-thick GO membrane on AAO. Compared with the AAO support (Fig. 1F), a very thin GO coating can be seen. We deposited a relatively thick GO membrane [~180 nm (Fig. 1G)] to correlate the GO deposition with the membrane thickness. GO dispersion for this 180-nm–membrane preparation was then diluted 100, 20, and 10 times to obtain the above 1.8-, 9-, and 18-nm-thick GO membranes, respectively, assuming no GO loss during filtration and constant membrane density. We used x-ray photoelectron spectroscopy (XPS) to detect surface elements for these ultrathin GO membranes on AAO (Fig. 1, H and I). For a 1.8-nm-thick membrane, a substantial amount of aluminum can be seen, because the mean free path of excited electrons is longer than the surface GO membrane thickness. However, for thicker membranes (9 and 18 nm), much smaller amounts of the underlying aluminum can be seen, because GO thickness is larger than the excited electron mean free path. This finding is consistent with surface carbon detection by XPS as well (Fig. 1I). See the supplementary materials for a detailed analysis.

We conducted permeation tests with different light gas molecules to probe pore sizes. Hydrogen (kinetic diameter: 0.289 nm) permeated ~300 times faster than did CO_2 (0.33 nm) through a ~18-nm-thick GO membrane at 20°C (Fig. 2A). Their kinetic diameter difference is only 0.04 nm, suggesting that the average size of pores for permeation in the GO membrane may be between 0.289 and 0.33 nm. O_2 and N_2 showed similar permeance as CO_2. However, CO and CH_4 had slightly higher permeance, although these molecules are are slightly larger than the aforementioned ones. Koenig *et al*. (*12*) also found that CH_4 had slightly higher permeance than N_2 through pristine graphene flakes, though the reason is still unclear. Figure 2B shows H_2 and He permeances for GO membranes with different thicknesses. Gas permeance is usually inversely proportional to the membrane thickness for conventional membranes (*14*). Surprisingly, we found that H_2 and He permeances decrease exponentially as membrane thickness increases from 1.8 to 180 nm (Fig. 2B). We speculate that the major transport pathway for these molecules is selective structural defects within GO flakes, instead of spacing between GO flakes. Reduction has been shown as an effective way to narrow interlayer spacing in GO membranes and, thus, limit permeation of molecules through spacing (*10*). We reduced GO membranes with thickness from 1.8 to 20 nm and conducted pressure-driven water permeat ion. We found that water permeance decreased approximately three orders of magnitude: For example, water permeance through a 3-nm GO membranes was 1370 liters/(m^2·hour·bar), whereas it was 0.5 to 1 liters/(m^2·hour·bar) through

[1]Department of Chemical Engineering, University of South Carolina, Columbia, SC 29208, USA. [2]Catalysis for Renewable Fuels Center, University of South Carolina, Columbia, SC 29208, USA. [3]Gas Technology Institute, 1700 South Mount Prospect Road, Des Plaines, IL 60018, USA. [4]College of Applied Science and Technology, Rochester Institute of Technology, Rochester, NY 14623, USA.

*Corresponding author. E-mail: yumiao@cec.sc.edu

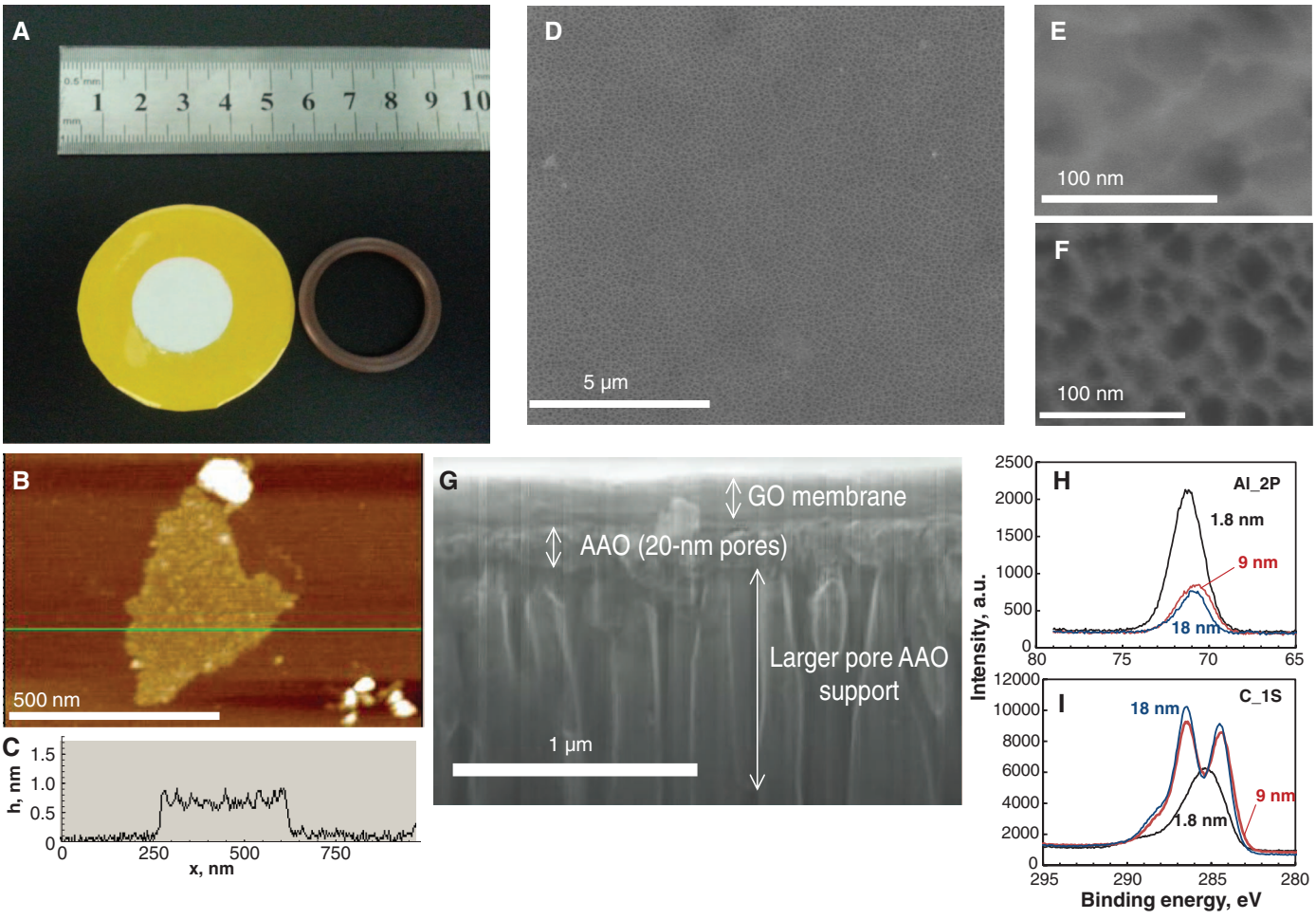

Fig. 1. GO membranes supported on porous AAO. (**A**) Digital picture of an ultrathin GO membrane on AAO (~9 nm). The white circular area is the permeation area (~4 cm^2) with supported GO; the yellow Kapton tape is used for GO protection and sealing by an O-ring during permeation measurements. (**B**) AFM image of a GO flake on freshly cleaved mica. (**C**) The height profile across the green line in (B) is shown here. h, height; x, position. (**D**) Field-emission scanning electron microscopy (FE-SEM) image of the surface of a GO membrane (~18 nm thick) on porous AAO. (**E**) FE-SEM image of the GO membrane surface (~18 nm thick) with higher magnification. (**F**) FE-SEM image of the AAO surface without the GO membrane. (**G**) FE-SEM image of the cross-sectional view of a thick GO membrane (~180 nm). (**H**) Al 2P and (**I**) C 1S XPS spectra of ultrathin GO membranes (~1.8, 9, and 18 nm thick) supported on porous AAO. a.u., arbitrary units.

a reduced GO membrane. This observation is in agreement with the findings of Nair *et al*. (*10*) and suggests that interlayer spacing has been eliminated or considerably narrowed by reduction. We then measured single-gas permeation through 18-nm reduced GO membranes (fig. S5) but found no obvious gas permeance change, which suggests that interlayer spacing is not the major transport pathway and permeation of molecules is attributed to the selective structural defects within GO flakes. Exponential dependence of gas permeances on membrane thickness (Fig. 2B) may result from the particular molecular transport pathway through the selective structural defects in layered GO membranes. Various defects on graphene have been found capable of separating H_2 from other small molecules (N_2, CH_4, etc.) (*15*–*17*). The molecular-sieving behavior of H_2 over other molecules may be attributed to the intrinsic defects in our membranes, as supported by the Raman spectrum [fig. S6 and analysis in (*13*)]. Koenig *et al*.

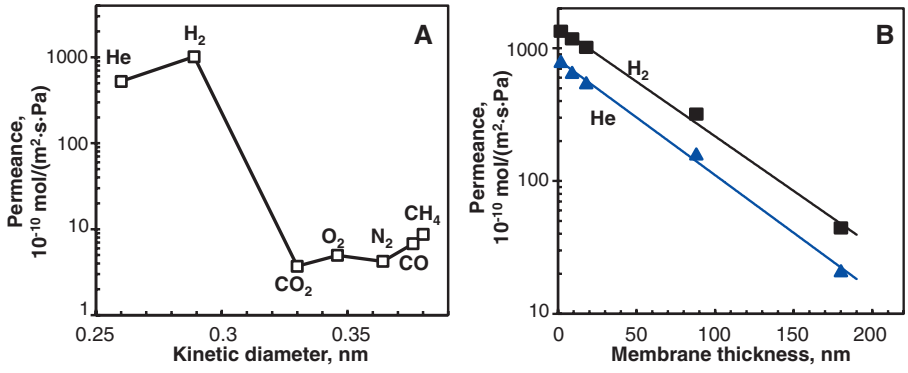

Fig. 2. Single-gas permeation through GO membranes supported on porous AAO at 20°C. (**A**) Permeances of seven molecules through a ~18-nm-thick GO membrane. (**B**) Permeances of H_2 and He through GO membranes with different thicknesses. The lines in (B) denote exponential fits.

(*12*) found that H_2/N_2 ideal selectivity for isolated graphene sheets was higher than 10,000 after etching graphene by ultraviolet-induced oxidation. We noticed that, before etching, some of their graphene sheets showed high ideal selectivities for H_2/CH_4 (~100) and H_2/N_2 (~100), indicating that intrinsic

defects may also have decent molecular-sieving behavior. Our single-gas permeation results were consistent with their observation. We also used an exponential fit to extrapolate He permeance for a 1-μm-thick GO membrane (see Fig. 2B) and found that it is, appropriately, 10^{-16} mol/(m^2·s·Pa). This explains why the 1-μm-thick GO membranes prepared by Nair *et al*. were impermeable to He (*10*). Separation of H_2 from other small molecules has important applications, such as precombustion CO_2 capture and H_2 recovery for ammonia production (*18*–*21*).

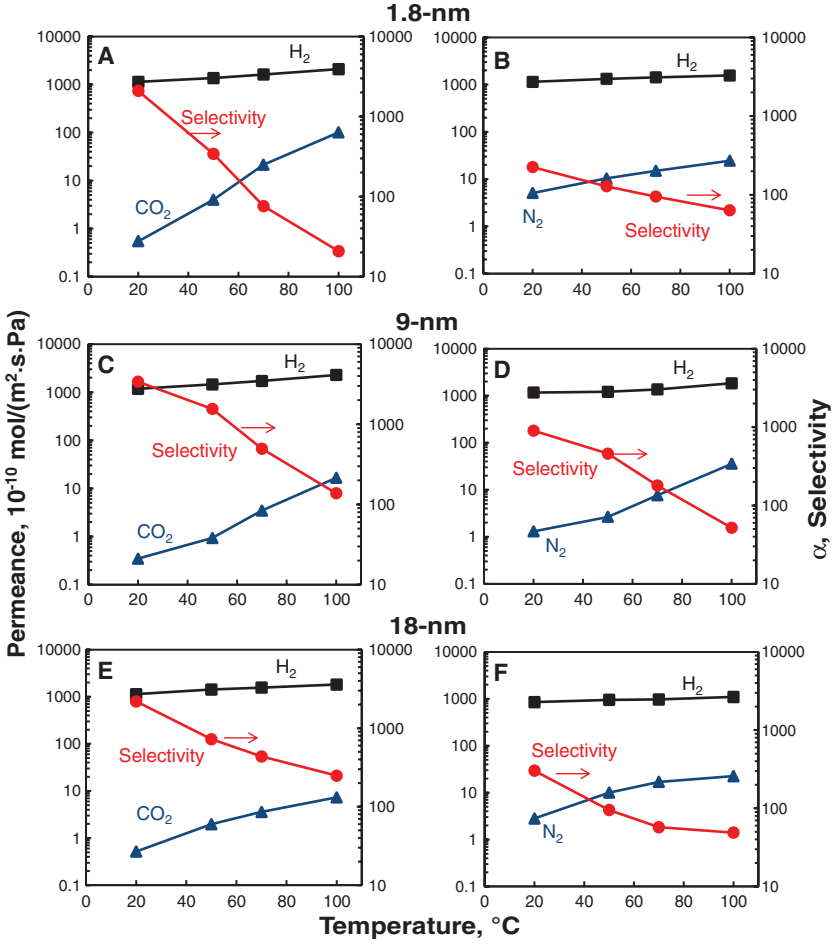

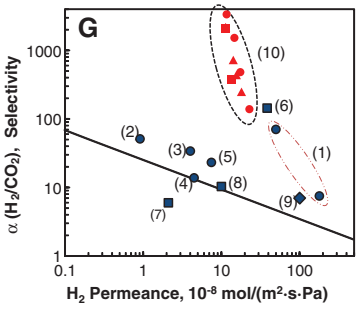

No.	Symbol	Membrane material	Temperature range, °C	Reference
1	●	Silica		(3)*
2	●	Silicon carbide		(26)
3	●	MFI Zeolite (modified)	100-300	(27)
4	●	ZIF-7		(28)
5	●	Zeolite composite		(29)
6	■	MFI zeolite (modified)		(30)
7	■	DDR zeolite	>300	(31)
8	■	Silica-titania		(32)
9	◆	MOF	<100	(33)
10	■ ● ▲	GO (1.8-nm) GO (9-nm) GO (18-nm)	20-100	this work

*Ideal selectivities and single gas permeances of H_2 from the reference

Fig. 3. 50:50 H_2/CO_2 and H_2/N_2 gas mixture separations and comparison with literature data. (**A**) and (**B**) show separation results for a 1.8-nm-thick GO membrane, (**C**) and (**D**) for 9-nm membrane, and (**E**) and (**F**) for an 18-nm membrane. (**G**) Comparison of ultrathin GO membranes with polymeric membranes and inorganic microporous membranes for H_2/CO_2 mixture separation: selectivity versus H_2 permeance. The black line denotes the 2008 upper bound of the polymeric membrane for H_2/CO_2 (*25*), assuming membrane thickness is 0.1 μm. Blue points (1 to 9) represent microporous inorganic membranes from the literatures (*3*, *26*–*33*); red points (10) indicate ultrathin GO membranes from this study. The table at right explains points 1 through 10. ZIF, zeolitic imidazolate framework; MOF, metal-organic framework.

Separation selectivity and permeance are two important parameters to evaluate membrane separation performance. We first conducted a control experiment for an AAO support. We found that the gas permeances were high [>10^{-6} mol/(m^2·s·Pa)] and selectivities of H_2 over CO_2 and N_2 were low (<5), as expected for Knudsen diffusion through 20-nm pores. Figure 3 shows separation results for 50:50 H_2/CO_2 and 50:50 H_2/N_2 mixtures for 1.8-, 9-, and 18-nm thick GO membranes. All the GO membranes showed high H_2/CO_2 selectivity (>2000) at 20°C, with a value of 3400 for the 9-nm-thick membrane. This is unusual, because microporous membranes reported in the literature showed low H_2/CO_2 selectivity (<10) or were selective to CO_2 over H_2 at temperatures below 100°C due to strong CO_2 adsorption and blocking of H_2 permeation (*22*–*24*). Adsorption isotherms on GO powder at 20°C showed much stronger CO_2 adsorption than H_2 adsorption (fig. S7). These results suggest a molecular-sieving separation of H_2 from CO_2, because strongly adsorbed CO_2 on GO flakes has negligible effects on H_2 permeation, which means that CO_2 cannot fit into most of the GO structural defects that only allow H_2 permeation. CO_2 seems to permeate through a very small number of larger structural defects. The observed H_2/CO_2 separation selectivity was higher than the ideal selectivity, implying that the larger defects are also selective for H_2 over CO_2, probably due to the smaller size of H_2. H_2/CO_2 separation selectivity decreased with increasing temperature, resulting from the faster increase of CO_2 permeance than that of H_2. But even at 100°C, H_2/CO_2 selectivity was still 250 for the 18-nm-thick membrane. This suggests a more activated CO_2 diffusion than that of H_2 through GO membranes, resulting from the tight fit of CO_2 molecules in these defects [fig. S8 and analysis in (*13*)]. H_2/N_2 mixture separation showed a similar behavior, and the highest selectivity is ~900 for the 9-nm GO membrane at 20°C. We have prepared at least three GO membranes for each thickness and obtained good reproducibility; variation of membrane permeation performance is within 15% for all membranes. We also fabricated ultrathin GO membranes on low-cost cellulous acetate supports (100-nm pores) and obtained similar separation performance. For example, for a ~18-nm-thick GO membrane on cellulous acetate support, H_2/CO_2 and H_2/N_2 separation selectivities are 1110 and 300, respectively. Figure 3G shows a comparison of ultrathin GO membranes with polymeric membranes and inorganic membranes for H_2/CO_2 mixture separation. Typically, for separation using polymeric membranes, permeance decreases as separation selectivity increases. An upper bound can typically be used to compare the separation performance of a new membrane with that of previous membranes. Ultrathin GO membranes are far above the upper bound for polymeric membranes (black line) and show superior separation performance compared with representative

inorganic membranes. Figure S9 shows the comparison of GO membranes with polymeric membranes for H_2/N_2 mixture separation, demonstrating the superior separation performance of GO membranes.

In summary, gas separation membranes, down to 1.8 nm in thickness, were reproducibly fabricated by a facile filtration method. These membranes showed H_2/CO_2 and H_2/N_2 mixture separation selectivities that are one to two orders of magnitude higher than those of the state-of-the-art microporous membranes. The fabrication of membranes on a low-cost polymer support was also demonstrated, making them attractive for the practical H_2 separation from mixtures.

References and Notes

1. Z. P. Lai *et al.*, *Science* **300**, 456–460 (2003).
2. M. Yu, R. D. Noble, J. L. Falconer, *Acc. Chem. Res.* **44**, 1196–1206 (2011).
3. R. M. de Vos, H. Verweij, *Science* **279**, 1710–1711 (1998).
4. M. B. Shiflett, H. C. Foley, *Science* **285**, 1902–1905 (1999).
5. H. B. Park *et al.*, *Science* **318**, 254–258 (2007).
6. D. A. Dikin *et al.*, *Nature* **448**, 457–460 (2007).
7. S. S. Chen *et al.*, *Am. Chem. Soc. Nano* **5**, 1321–1327 (2011).
8. C. Lee, X. D. Wei, J. W. Kysar, J. Hone, *Science* **321**, 385–388 (2008).
9. J. S. Bunch *et al.*, *Nano Lett.* **8**, 2458–2462 (2008).
10. R. R. Nair, H. A. Wu, P. N. Jayaram, I. V. Grigorieva, A. K. Geim, *Science* **335**, 442–444 (2012).
11. O. Leenaerts, B. Partoens, F. M. Peeters, *Appl. Phys. Lett.* **93**, 193107 (2008).
12. S. P. Koenig, L. Wang, J. Pellegrino, J. S. Bunch, *Nat. Nanotechnol.* **7**, 728–732 (2012).
13. See supplementary materials on *Science* Online.
14. S. T. Oyama, D. Lee, P. Hacarlioglu, R. F. Saraf, *J. Membr. Sci.* **244**, 45–53 (2004).
15. D. E. Jiang, V. R. Cooper, S. Dai, *Nano Lett.* **9**, 4019–4024 (2009).
16. H. L. Du *et al.*, *J. Phys. Chem. C* **115**, 23261–23266 (2011).
17. X. Qin, Q. Y. Meng, Y. P. Feng, Y. F. Gao, *Surf. Sci.* **607**, 153–158 (2013).
18. N. W. Ockwig, T. M. Nenoff, *Chem. Rev.* **107**, 4078–4110 (2007).
19. P. Bernardo, E. Drioli, G. Golemme, *Ind. Eng. Chem. Res.* **48**, 4638–4663 (2009).
20. A. Brunetti, F. Scura, G. Barbieri, E. Drioli, *J. Membr. Sci.* **359**, 115–125 (2010).
21. C. A. Scholes, K. H. Smith, S. E. Kentish, G. W. Stevens, *Int. J. Greenh. Gas Control* **4**, 739–755 (2010).
22. M. Hong, S. G. Li, J. L. Falconer, R. D. Noble, *J. Membr. Sci.* **307**, 277–283 (2008).
23. G. Q. Guan, T. Tanaka, K. Kusakabe, K. I. Sotowa, S. Morooka, *J. Membr. Sci.* **214**, 191–198 (2003).
24. T. Tomita, K. Nakayama, H. Sakai, *Microporous Mesoporous Mater.* **68**, 71–75 (2004).
25. L. M. Robeson, *J. Membr. Sci.* **320**, 390–400 (2008).
26. B. Elyassi, M. Sahimi, T. T. Tsotsis, *J. Membr. Sci.* **288**, 290–297 (2007).
27. M. Hong, J. L. Falconer, R. D. Noble, *Ind. Eng. Chem. Res.* **44**, 4035–4041 (2005).
28. Y. Li, F. Liang, H. Bux, W. Yang, J. Caro, *J. Membr. Sci.* **354**, 48–54 (2010).
29. M. Yu, H. H. Funke, R. D. Noble, J. L. Falconer, *J. Am. Chem. Soc.* **133**, 1748–1750 (2011).
30. Z. Tang, J. Dong, T. M. Nenoff, *Langmuir* **25**, 4848–4852 (2009).
31. M. Kanezashi, J. O'Brien-Abraham, Y. S. Lin, K. Suzuki, *AIChE J.* **54**, 1478–1486 (2008).
32. Y. Gu, S. T. Oyama, *J. Membr. Sci.* **345**, 267–275 (2009).
33. H. Guo, G. Zhu, I. J. Hewitt, S. Qiu, *J. Am. Chem. Soc.* **131**, 1646–1647 (2009).

Acknowledgments: We thank the University of South Carolina for start-up funding, S. Ma for experimental assistance on XPS, C. T. Williams for assistance with Raman spectroscopy, and J. R. Regalbuto for suggestions on writing the manuscript. M.Y. and H.L. are inventors on U.S. patent application number 61/850,415 ("Ultrathin, Molecular-Sieving Graphene Oxide Membranes for Separations"), applied for by the University of South Carolina.

Supplementary Materials

www.sciencemag.org/content/342/6154/95/suppl/DC1
Materials and Methods
Supplementary Text
Figs. S1 to S9
References (*34*–*40*)

18 February 2013; accepted 28 August 2013
10.1126/science.1236686

Specific Chemical Reactivities of Spatially Separated 3-Aminophenol Conformers with Cold Ca^+ Ions

Yuan-Pin Chang,[1]* Karol Długołęcki,[1] Jochen Küpper,[1,2,3]† Daniel Rösch,[4]* Dieter Wild,[4] Stefan Willitsch[4]†

Many molecules exhibit multiple rotational isomers (conformers) that interconvert thermally and are difficult to isolate. Consequently, a precise characterization of their role in chemical reactions has proven challenging. We have probed the reactivity of specific conformers by using an experimental technique based on their spatial separation in a molecular beam by electrostatic deflection. The separated conformers react with a target of Coulomb-crystallized ions in a trap. In the reaction of Ca^+ with 3-aminophenol, we find a twofold larger rate constant for the cis compared with the trans conformer (differentiated by the O–H bond orientation). This result is explained by conformer-specific differences in the long-range ion-molecule interaction potentials. Our approach demonstrates the possibility of controlling reactivity through selection of conformational states.

Recent progress in the cooling, manipulation, and control of isolated molecules in the gas phase (*1*–*4*) has paved the way for the study of chemical processes at high levels of sensitivity, selectivity, and detail. Methods for slowing and merging of supersonic molecular beams have enabled precise characterizations of the role of collision energy and of the molecular quantum state in scattering and reactive processes (*5*–*7*). Recent experiments with trapped, translationally cold molecules and ions have provided insights into the quantum dynamics of chemical reactions (*8*) and the subtleties of intermolecular interactions (*9*). These experiments have thus far been restricted to reactions involving atoms or small molecules with simple geometric and quantum structures. The vast majority of molecules, however, possess a plethora of internal degrees of freedom that are challenging to probe independently. In particular, polyatomic molecules usually exhibit many rotational isomers (conformers) that interconvert with low thermal barriers through rotations about covalent bonds. Recent years have seen impressive progress in the spectroscopic characterization of specific conformations (*10*–*12*), their photoinduced isomerization (*13*, *14*), and the characterization of conformer-specific photodissociation dynamics (*15*, *16*). However, studies of specific conformational effects in bimolecular reactions are still sparse (*17*, *18*), in particular in the gas phase, where the highest degree of control and therefore insight into fundamental reaction mechanisms can be gained.

Here, we introduce a distinct approach for the study of conformational effects and conformation-dependent reactivities, that is, rate constants, in bimolecular reactions. Our method exploits the spatial separation of different conformers by using inhomogeneous electric fields (*19*, *20*). Internally cold molecules in a beam are dispersed by an electrostatic deflector and are directed toward the reaction volume. There, they interact with laser-cooled ions in a Coulomb crystal, that is, an ordered structure of translationally cold ions in a trap (*4*). The Coulomb crystal constitutes a tightly localized, stationary reaction target much smaller in extension than the conformationally separated regions of the beam so that chemical reactions can be studied selectively with isolated conformers.

We studied the reaction of individual conformers of 3-aminophenol (AP) with Ca^+ ions to

[1]Center for Free-Electron Laser Science, DESY (Deutsches Elektronen-Synchrotron), Notkestrasse 85, 22607 Hamburg, Germany. [2]The Hamburg Center for Ultrafast Imaging, University of Hamburg, Luruper Chaussee 149, 22761 Hamburg, Germany. [3]Department of Physics, University of Hamburg, Luruper Chaussee 149, 22761 Hamburg, Germany. [4]Department of Chemistry, University of Basel, Klingelbergstrasse 80, 4056 Basel, Switzerland.

*These authors contributed equally to this work.
†Corresponding author. E-mail: jochen.kuepper@cfel.de (J.K.); stefan.willitsch@unibas.ch (S.W.)